Cellulose (2018) 25:3327–3337
https://doi.org/10.1007/s10570-018-1803-6

ORIGINAL PAPER

# Binding preference of family 1 carbohydrate binding module on nanocrystalline cellulose and nanofibrillar cellulose films assessed by quartz crystal microbalance

**Yu Zhang · Fang Yang · Fanghui Hu · Junlong Song · Shufang Wu · Yongcan Jin**

Received: 5 November 2017 / Accepted: 20 April 2018 / Published online: 23 April 2018


**Abstract** It is important to understand the interactions between the carbohydrate-binding module of fungal cellulases (CBM1) and the surface of cellulose because those interactions play an important role in the degradation of the crystalline regions of cellulose. In this investigation, interactions between isolated CBM1 and nanofibrillar and nanocrystalline cellulose (NFC and NCC, respectively) films were monitored with a quartz crystal microbalance with dissipation (QCM-D) in situ and in real time. The adsorption isotherms were employed to obtain the thermodynamic parameters of the interactions. Both Langmuir and Freundlich models appropriately describe the adsorption process of CBM1 on both types of films. Values of the Gibbs free energy associated with the adsorption of CBM1 on the NCC and NFC films were − 25.6 and − 23.7 kJ/mol, respectively. The results implied that the CBM1 binds spontaneously to both films but preferentially to NCC, with the differences attributed to variations in crystallinity and porosity of these substrates.

**Keywords** Carbohydrate binding module (CBM) · Nanofibrillar cellulose (NFC) · Nanocrystalline cellulose (NCC) · Adsorption · Quartz crystal microbalance (QCM) · Thermodynamic evaluation

## Introduction

The interaction between cellulolytic enzymes and their substrates is of central importance to several technological and scientific challenges because it plays an important role in converting pretreated solid cellulosic materials into soluble fermentable sugars (Hervé et al. 2010; Nussinovitch et al. 2002). Specific interaction between cellulases and cellulose may generate some advanced materials (Laaksonen et al. 2011; Mittal et al. 2017). A typical cellulolytic enzyme contains one catalytic domain (CD) and one or more cellulose binding domains (CBDs) or modules (CBMs) connected by an inter-domain linker peptide (Linder and Teeri 1997; Mattinen et al. 1997). The primary function of CBMs is to facilitate the association of the parent enzyme with the substrate. This involves targeting the enzyme to the appropriate substrate and increasing the local concentration of the enzyme and hence enhancing enzyme activity (Eriksson et al. 2005; McGuffee and Elcock 2006; Mittal et al. 2011; Notenboom et al. 2001). According to the amino acid sequence similarity and the 3D structure of binding module, cellulases are classified

Yu Zhang and Fang Yang have contributed equally.

Y. Zhang · F. Yang · F. Hu · J. Song (✉) · S. Wu · Y. Jin
Jiangsu Co-Innovation Center for Efficient Processing and Utilization of Forest Resources, Nanjing Forestry University, Nanjing 210037, China
e-mail: junlong.song@njfu.edu.cn

into more than 70 families (http://www.cazy.org/CBM1_all.html). CBM1 is the CBM from family 1 and is found almost exclusively in fungi. CBM1 consists of 36 amino acid residues and exhibits a wedge-shaped structure (Linder and Teeri 1997; Mattinen et al. 1997).

Numerous experiments have been performed to understand the interactions between CBM and cellulose substrate using different techniques, such as electron microscopy (Lehtio et al. 2003), single molecule fluorescence (Dagel et al. 2011), and atomic force microscopy (Liu et al. 2011), suggesting that the CBM of Family 7 cellobiohydrolase from *Trichoderma reesei* (CBM-Cel7A, one type of CBM1) binds preferentially to the hydrophobic faces of cellulose Iα. Palonen et al. (1999) found that enzyme affinity is also relevant to the linkage between CDs and CBMs and Cel6A and Cel7A are different in binding reversibility. The research conducted by Arola and Linder (2016) demonstrated that the substrate has a great impact on the exchange rate of the CBM. The CBM-Cel7A appears to have different modes of binding on wood derived cellulose from cellulose originating from bacterial source.

Computer simulation sheds some light on the detailed mechanisms of CBM-cellulose interactions. Yui et al. (2010) conducted a computer docking study using combined Brownian dynamics (BD) and molecular dynamics (MD) simulations. The study suggested that the CBM-Cel7A binds preferentially to the hydrophobic faces of cellulose Iα. Alekozai et al. (2014) characterized the binding of CBM to the cellulose Iβ fiber. Their results confirmed that CBM prefers to dock to the hydrophobic than to the hydrophilic fiber faces, revealing that both electrostatic (ES) and van der Waals (VDW) interactions are required for achieving the observed binding preference. Beckham et al. (2010) built a fully atomistic model and probed the molecular-level behavior of CBM-Cel7A on the hydrophobic face of crystalline cellulose. They found that the CBM can anchor the Cel7A enzyme at discrete points along a cellulose chain and thus aid in both recognizing cellulose chain ends for initial attachment to cellulose as well as aid in enzymatic catalysis by diffusing between stable wells on a length scale commensurate with the catalytic, processive cycle of Cel7A during cellulose hydrolysis. They determined the residues that are responsible for the observed processivity length scale of the CBM: Y5, Q7, N29, and Y32. Nimlos et al. (2012) demonstrated that there is a thermodynamic driving force for CBM-Cel7A to bind preferentially to the hydrophobic surface of cellulose relative to hydrophilic surfaces. In addition, their simulations demonstrated that the CBM can diffuse from hydrophilic surfaces to the hydrophobic surface, whereas the reverse transition is not observed.

However, the nature of the CBM-cellulose binding is still not well understood. Creagh et al. (1996) concluded that the binding of the CBM of the exoglucanase Cex from *Cellulomonas fimi* to insoluble crystalline cellulose is entropically driven. In the work by Boraston (2005), however, it was suggested that the interaction of the CBM with non-crystalline cellulose is mainly enthalpically driven. The exact role of the CBM in the hydrolysis of crystalline cellulose remains to be elucidated (Alekozai et al. 2014; Hu et al. 2018).

Adsorption is a reflection of the interfacial properties. Many adsorption theories including Henry adsorption theories, Freundlich adsorption theories, Langmuir adsorption theories and BET adsorption theories are applied to fit the adsorption data (Tsiamis and Taylor 2017). Freundlich and Langmuir adsorption theories are often used to describe the interactivity between CBM and cellulose (Pellegrini et al. 2014; Seo et al. 2011; Xu et al. 2013). Based on the adsorption isotherms, the thermodynamics of CBM-cellulose can be assessed. To evaluate the thermodynamics of CBM-substrate, isothermal titration calorimetry (ITC) was performed essentially for soluble oligosaccharides (Boraston et al. 2002, 2003; Flint et al. 2004; Lammerts van Bueren and Boraston 2004; Sakka et al. 2003). The binding isotherms of CBM from different origins were performed by $^{3}$H-labled protein (Arola and Linder 2016) and affinity electrophoresis (Tomme et al. 2000) as well. Based on the thermodynamics evaluated by titration, free energy diagram for the heterogeneous enzymatic hydrolysis of glycosidic bonds in cellulose was established by Sorensen et al. (2015a, b).

The traditional analytical methods are able to detect only the final products of the interactions between CBM/cellulase and substrate, but they are not able to monitor the adsorption process dynamically and in real time. Recently, quartz crystal microbalance (QCM) has become a very useful method for studying the interfacial phenomena in different scientific fields (Ahola et al. 2008a, b; Hu et al. 2009, 2018; Jiang et al.

2017; Josefsson et al. 2007; Turon et al. 2008). Quartz crystal microbalance with dissipation (QCM-D) technique can give in situ information about the adsorption kinetics and adsorption mass as well as the viscoelastic properties of the adlayer at the solid/liquid interface (Fält et al. 2003; Martin-Sampedro et al. 2013; Rodahl et al. 1995; Shen et al. 2016; Song et al. 2017; Tammelin et al. 2006, 2007).

Our study was to identify the impact of supramolecular arrangement of cellulose chains on the binding preference of CBM. The interactions between the isolated CBM1 and nanocrystalline cellulose (NCC) and nanofibrillar cellulose (NFC) films were investigated by QCM-D. Our study focused on only the CBM1, instead of the entire enzyme because the initial binding of enzyme to the substrate is mainly mediated by the CBM (Boraston et al. 2004; Guillen et al. 2010; Hervé et al. 2010). It has also been shown experimentally that an isolated CBM can bind to cellulose crystals (Dagel et al. 2011; Lehtio et al. 2003; Liu et al. 2011). Therefore, studying only the adsorption of CBM1 on substrates can eliminate the influences of the CD portion and the linker. The changes of the frequency and dissipation in QCM-D determined the conformational changes of the CBM1 adlayer on NFC and NCC films under the different concentrations. The adsorption isotherms of CBM1 on the two substrates were described by Langmuir and Freundlich models. The binding preference was assessed by thermodynamic parameters.

## Experimental

### Materials

CBM1 was obtained from Nzytech Corp. (Ribbens, Portugal). Microcrystalline cellulose was provided by Sinopharm Chemical Reagent Co., Ltd. (Shanghai, China). Polyethyleneimine (PEI, Mw = $7.5 \times 10^5$, 50 wt% in $H_2O$) solution was purchased from Sigma-Aldrich Co., Ltd. (Shanghai, China). Other chemicals were ordered from Nanjing Chemical Reagent Co., Ltd. (Nanjing, China). All chemicals were used as received. QCM-D sensors with silica surface were supplied by Q-Sense AB (Biolin Scientific Co. Ltd, Sweden).

### Modification of QCM sensors with NFC/NCC films

Nanofibrillar cellulose (NFC) films were prepared using the method adopted from Ahola et al. (2008a). The NFC was obtained from the microfluidization (M110P Microfluics Corp., Newton, U.S.) of bleached sulphite birch pulp. It ($\sim$ 0.1 wt% NFC in Milli-Q-water) was dispersedly spin-coated (WS-650SX-6NPP spin coater, Laurell Technologies, North Wales, PA, USA) at 3000 r/min on QCM crystals with a pre-adsorbed polyethyleneimine (PEI) layer. The NFC-coated QCM crystals were stored in a desiccator until use. Prior to QCM-D measurements, the NFC-surfaces were allowed to stay overnight in buffer solution.

The procedures of nanocrystalline cellulose (NCC) film preparation were addressed in detail elsewhere (Jin et al. 2016, 2017). Pristine NCC was initially hydrolyzed from microcrystalline cellulose by sulfuric acid followed the method described previously (Beck-Candanedo et al. 2005). The obtained cellulose suspension contained mainly nano-sized cellulose crystals with polymorph I. The contents were then neutralized and dialyzed with cellulose dialysis film with MWCO 14000 until the conductivity reached a constant close to pure water. QCM sensors coated with NCC were prepared followed the same procedures as addressed in NFC film.

By comparing the frequency drop before and after film deposition, the thickness of NFC and NCC films on QCM sensors was calculated to be in the range of 26–29 and 19–21 nm, respectively, given that the density of films was 1400 kg/m$^3$ and the porosity of films was $\sim$ 10% (Niinivaara et al. 2015).

### Characterization of NFC and NCC films

The morphology of NFC and NCC films on QCM sensors was characterized using an atomic force microscopy (AFM, Dimension Edge, Brucker Co., Ltd., Germany). Images were obtained in a tapping mode by commercial silicon cantilevers with a spring constant of 20–80 N/m and a resonance frequency of 300–340 kHz. The scan size of $5 \times 5$ or $2 \times 2$ μm$^2$ was conducted and images were scanned at least three different locations on each sample. The obtained images were flattened without further modifications.

Adsorption of CBM1 under different concentrations on model cellulose films monitored by Quartz Crystal Microbalance with Dissipation (QCM-D) technique

The CBM1 solutions with a range of concentrations (100, 80, 60, 40, 20 ppm based on protein content) in acetic acid/sodium acetate buffer (0.1 M, pH 4.8) were prepared initially. The NFC and NCC coated QCM sensors were mounted in the chambers and the buffer was loaded to remove impurities of the surfaces and stabilized the films. The temperature in the chambers was kept at 25 °C during the entire measurements. CBM1 solutions with two different concentrations were loaded into four chambers of QCM at the rate 0.1 mL/min for 10 min after the QCM system was stabilized. Each experiment was repeated at least twice. The resulting frequency and dissipation changes of QCM crystals at 5 MHz fundamental resonance frequency and their 3rd, 5th, 7th, 9th, and 11th overtone data were recorded. The pump was not restarted (at a constant flow rate of 0.1 mL/min) with the buffer solution to flush the system until the frequency and dissipation values reached a steady state.

## Results and discussion

The characterizations of NFC and NCC films

The morphology of NFC and NCC films coated on QCM sensors was shown in Fig. 1a, b, respectively. It appeared that both cellulose covered the entire surface of the sensors. It is known that NFC has multiscale characteristics ranging from their nano-structure to macro-structure (Song et al. 2017). It was observed that nanofibrils were evenly distributed on the sensor surfaces and some fibril bundles were present but in a relatively small amount. The width of the cellulose nanofibrils was in the range of 30–100 nm and the voids between nanofirbrils exhibited diameters of 10–200 nm. In the case of NCC, the film was smoother than NFC film. A number of needle-like whiskers with a size of around 10 nm in width and 100–300 nm in length were found evenly on QCM sensors, forming a compact layer on silica sensors. Both NFC and NCC films exhibited porous structures due to the rigid nature of NFC and NCC as well as the cross-linked

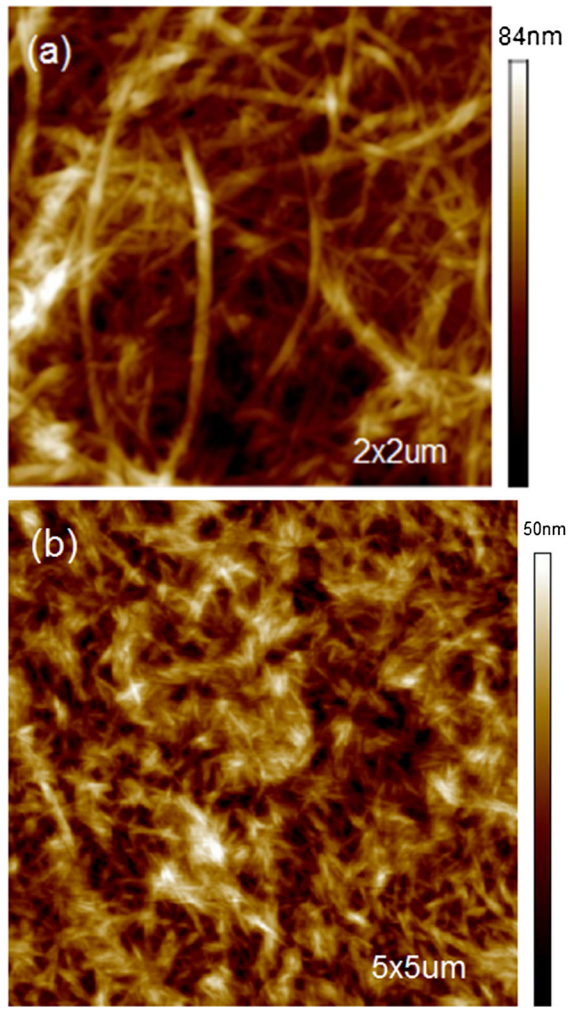


**Fig. 1** The AFM images of **a** NFC and **b** NCC films coated on QCM sensors

network. The surface roughness (expressed in RMS) of NCC and NFC films was 4.7–5.0 and 5.0–5.6 nm, respectively. The results are in good agreement with our previous observations (Hu et al. 2018; Jin et al. 2017; Song et al. 2017).

The adsorption behaviors of CBM1 on the substrates of NFC and NCC monitored by QCM

The adsorption behaviors of CBM1 on NFC and NCC substrates were monitored by QCM-D in situ and in real time. Figure 2a showed both frequency (left axis, data presented in solid symbols) and dissipation (right axis, data presented in open symbols) changed after

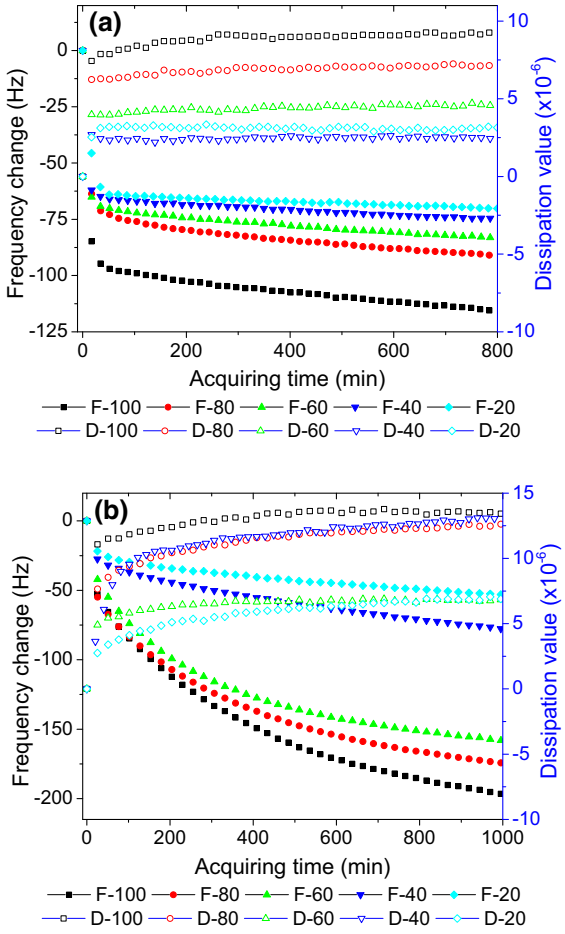


**Fig. 2** Frequency and dissipation changes after loading CBM1 with varied concentrations (20–100 ppm) on **a** NCC and **b** NFC model films

CBM1 loaded with different concentrations (100, 80, 60, 40, 20 ppm) on NCC film. Multiple overtone data were recorded in this investigation. Because all overtone data followed the similar trend and differed slightly, only the 3rd overtone data were reported in Fig. 2. It was seen that the adsorption of CBM1 on NCC surface developed quickly. Dissipation values reached their equilibrium state in less than 50 min for all five concentrations. The change in frequency consisted of two stages. The fast adsorption process suggested by a fast frequency drop, was finished in 50 min. However, after the fast adsorption process the frequencies continued to drop gradually even when the energy dissipation values reached their stable state. Because in general enzyme adsorption accomplishes quite fast, the slowed adsorption process observed in this study may be attributed to the diffusion of CBM in the cellulose film. In addition, it was found that a higher frequency drop and a higher dissipation value were gained by a higher concentration of CBM.

The adsorption curves of CBM1 with different concentrations (100, 80, 60, 40, 20 ppm) on NFC films were presented in Fig. 2b. The curves demonstrated distinct behaviors from those on NCC film. First, the adsorption mass of CBM1 on NFC film was much higher than that on NCC film, especially at a high concentration. Their frequency drops were more than double NCC film did. The corresponding energy dissipation values were in accord with the frequency change, to a higher value. Second, the time required to reach the stable state on NFC film was much more than that on NCC film. It was found that the dissipation values reached a stable state in about 600 min, while for all monitored frequency changes, they kept increasing till the end of experiments. It hints that the diffusion of CBM1 in NFC film is more pronounced than that observed on the NCC film. This is correlated and consistent with the porous structure and roughness of NFC and NCC films as shown in Fig. 1.

In order to elucidate the conformations of the adsorbed CBM1 layer on NCC and NFC films, the plots of frequency change against energy dissipation for each CBM1 concentration are shown in Fig. 3a, b, respectively. In Fig. 3a, all $\Delta D/\Delta f$ curves for different CBM1 concentrations exhibited the similar behavior: a straight slope for initial adsorption followed by a horizontal adsorption, at last a slope again. The slope for each concentration was quite similar at the initial adsorption, indicating that the conformations of CBM1 layer on NCC surface with different concentration were the same. At the second stage of horizontal adsorption, the frequency changed (mass increases), but the dissipation value of the adsorbed layer remained constant, suggesting that the adsorbed CBM1 layer became compact and a rearrangement of CBM1 conformation occurred in this stage. In addition, the thickness of CBM1 layer required for the conformation rearrangement correlated strongly with the CBM1 concentration. The conformation rearrangement in a thick CBM1 layer required a high CBM1 concentration. At the last stage of adsorption, a small slope is observed for all experiments in a comparison of the initial adsorption slope, indicating that the conformation of adsorbed CBM1 layer at the

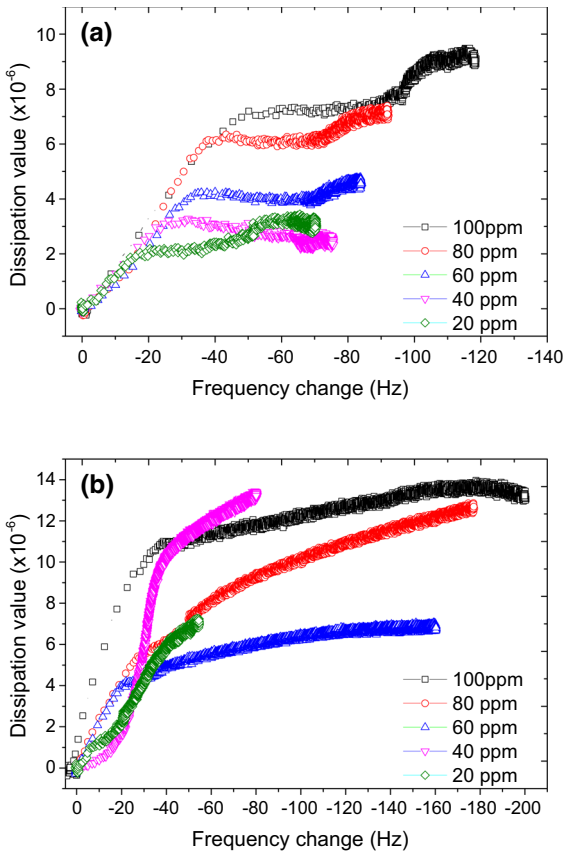


**Fig. 3** Plots of energy dissipation against frequency change of the adsorbed CBM1 layer on **a** NCC and **b** NFC model films

last stage was even more compact than that in the initial adsorption.

The plots of ΔD/Δf of adsorbed CBM1 layer for different CBM1 concentrations (100, 80, 60, 40, 20 ppm) on NFC film were shown in Fig. 3b. They exhibited quite different behaviors comparing those on the NCC film. A soft initial adsorption (steep slope) followed by a conformation rearrangement was observed for all concentrations. The slopes for different concentrations for initial adsorption did not overlap, unlike that on the NCC film. It may attribute to the heterogeneity of NFC film structure as shown in Fig. 1b.

## Adsorption isotherms

The adsorption isotherm is significant information that can represent the equilibrium process of the adsorbate molecules between liquid and solid phases (Hasan et al. 2008). Many kinds of isotherms can describe the equilibrium characteristics of adsorption. Langmuir and Freundlich adsorption isotherms are employed widely.

QCM-D measures frequency change and dissipation which units are different from those used in isothermal fitting. Sauerbrey equation suggests a relationship between the frequency change and the adsorbed mass (Sauerbrey 1959) (Eq. 1):

$$\Delta m = c\frac{\Delta f_n}{n} \tag{1}$$

where $n$ is the overtone number ($n$ = 1, 3, 5, and 7) and $c$ is a constant representing the mass sensitivity at 5 MHz. For the used crystals the mass sensitivity is − 0.177 mg m$^{-2}$Hz$^{-1}$ (Song et al. 2009, 2010). It is noted that the Sauerbrey relation does not apply to viscoelastic or soft adlayers because they may not fully couple with the motion of the sensor. The frequency change might be affected by the mechanical properties of the film such as shear modulus and viscosity. In such cases, Sauerbrey equation tends to underestimate the calculated mass and hence viscoelastic models such as Voigt model have been recommended in the study (Garg et al. 2008; Voinova et al. 1999). Here the viscoelastic system is conceptualized as a spring and dashpot corresponding to the elastic (storage) and inelastic (damping) behavior of the material. Energy loss (dissipation D) and frequency shift at different overtones are therefore collected and fitted to film viscosity, shear modulus, thickness, and density of the adsorbed layer using QTools software (Q-Sense). The method can be found elsewhere (Garg et al. 2008; Song et al. 2017; Voinova et al. 1999). The calculation of the mass of NCC and NFC in adsorption assumes that all the cellulose covered on QCM crystals involved in the adsorption process.

The equation of Langmuir isotherm can be expressed as Eq. 2.

$$Q_e = K_L \cdot C \cdot Q_m/(1 + K_L \cdot C) \tag{2}$$

where $Q_e$ is the amount of adsorbed CBM1 in equilibrium (expressed in frequency change, Hz, or calculated adsorption mass by QTools, nmol g$^{-1}$), $Q_m$ is the maximum amount of CBM1 which can be adsorbed on substrate (unit same as $Q_e$), $K_L$ is the

equilibrium adsorption constant (L $mol^{-1}$); $C$ (mg $L^{-1}$) is the equilibrium concentration of CBM1 in the solution.

The linear form of Langmuir isotherm is represented as Eq. 3.

$$1/Q_e = 1/Q_m + 1/(K_L \cdot C \cdot Q_m) \quad (3)$$

where $K_L$ and $Q_m$ can be obtained from the slope and intercept of Langmuir isotherm linear form.

The fitting of Langmuir isotherms of NCC and NFC at 25 °C is shown in Fig. 4a. The effectiveness of fit for the isotherms is rated by coefficient $r^2$. The results show that the coefficients of Langmuir isotherms for the adsorption of CBM1 on NFC and NCC films are all over 0.98, indicating a monolayer of CBM1 adsorbed on either NCC or NFC film. Langmuir constants $K_L$ and $Q_m$ are calculated from the figures and summarized in Table 1.

The adsorption mass of CBM1 on NFC film is significantly greater than that on NCC film at the same concentration. The values of $Q_m$ in Table 1 offer another confirmation that they are − 144.7 and − 482.3 Hz for NCC and NFC films, respectively, which are equivalent to 24.69 and 59.88 μmol $g^{-1}$. These latter two values expressed in traditional unit are apparently greater than those literature values reported previously. For example, Ciolacu et al. (2010) reported that the adsorption of cellulase on dissolving pulp, linters cellulose and cotton cellulose was in a range of 1.677–2.361 μmol $g^{-1}$ and it increased to 4.960–5.862 μmol $g^{-1}$ for cellulose fibers after polymorphic conversion (Ciolacu et al. 2014). It is apparent that the maximal adsorption amount of CBM is strongly correlated with the surface area of substrate accessible for adsorption. In our study, the cellulose substrates of both NCC and NFC are in nanoscale size. Therefore, it is reasonable that the $Q_m$ obtained from isotherms acquired by nanocellulose is greater than that obtained by macro fibers. If partial substrate had been considered in the calculation, a greater $Q_m$ value would be obtained. From this aspect, the great $Q_m$ obtained by QCM technique substantially supports our assumption that the entire layer of cellulose substrate on the QCM sensors is fully involved in the adsorption process because CBM1 can diffuse into the porous NCC and NFC films.

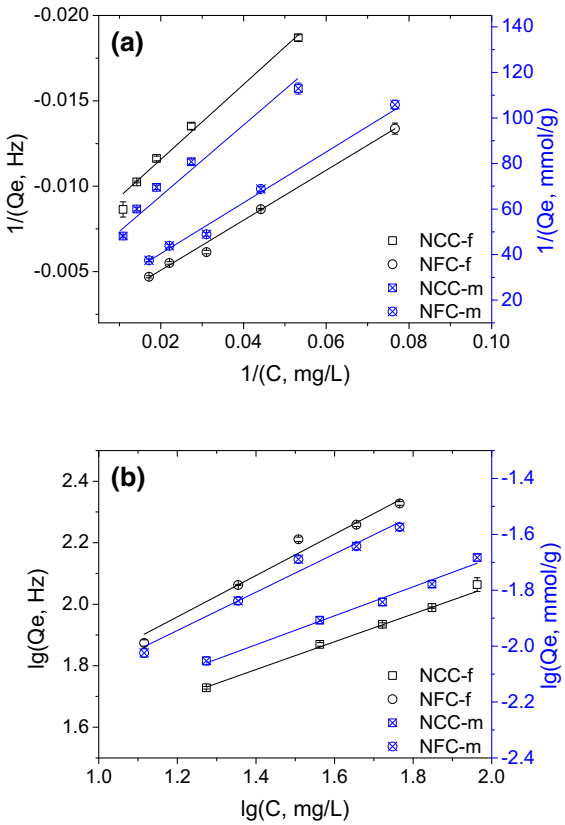


**Fig. 4** Isothermal adsorption of CBM1 on NFC and NCC films fitting by **a** Langmuir and **b** Freundlich models

A big difference is found in the $Q_m$ between NCC and NFC. It may be attributed to the accessible surface area of the films some extent. AFM images show that there are some large fiber bundles in the NFC film, resulting in a porous structure. The porous structure of NFC film offers a plenty of space for the CBM to access and hence a great adsorption capacity is achieved. On the other hand, although the size of NCC is small compared to NFC, the NCC film is compact as shown in Fig. 1, resulting in an adsorption capacity that is less than NFC but much higher than normal fibers.

$K_L$ derived from Langmuir model is 0.03056 and 0.01412 L $mg^{-1}$ for the adsorption of CBM1 on NCC and NFC ultrathin films, respectively when the adsorbed amount expressed in frequency. For comparison, $K_L$ is 0.03089 and 0.01441 L $mg^{-1}$, respectively, when the adsorbed amount expressed in mass. Obviously, the affinity parameter, $K_L$, derived from two sets of data expressed in frequency (left axis) and mass (right axis) is almost identical. The dissipation value acquired in this investigation was comparative

**Table 1** Isothermal adsorption models and fitting parameters

| Adsorption model | Substrate | Fitting equation | Fitting parameters | | |
|---|---|---|---|---|---|
| Langmuir | | | $Q_m$ (Hz) ($\mu$mol $g^{-1}$) | $K_L$ (L $mg^{-1}$) | $r^2$ |
| | NCC | $1/Q_e = -0.006909 - 0.2261/C$ | − 144.7 | 0.03056 | 0.984 |
| | | ($1/Q_e = 40.51 + 1311.24/C$) | (24.69) | (0.03089) | (0.997) |
| | NFC | $1/Q_e = -0.002073 - 0.1468/C$ | − 482.3 | 0.01412 | 0.994 |
| | | ($1/Q_e = 16.6990 + 1158.47/C$) | (59.88) | (0.01441) | (0.993) |
| Freundlich | | | $K_F$ (Hz $mg^{-1/n}L^{1/n}$) ($\mu$mol $g^{-1-1/n}L^{1/n}$) | 1/n | $r^2$ |
| | NCC | $lgQ_e = 0.4734lgC + 1.1246$ | 13.32 | 0.4734 | 0.996 |
| | | ($lgQ_e = 0.4777lgC - 2.6486$) | (2.246) | (0.4777) | (0.995) |
| | NFC | $lgQ_e = 0.7000lgC + 1.108$ | 12.91 | 0.7000 | 0.98 |
| | | ($lgQ_e = 0.6948lgC - 2.7818$) | (1.653) | (0.6948) | (0.98) |

low (no more than $14 \times 10^{-6}$), which was substantially lower than that formed by the entire enzymes ($\sim 40 \times 10^{-6}$) as addressed elsewhere (Song et al. 2017), suggesting the adlayer caused by CBM1 on cellulose substrate is quite compact or rigid. Therefore, the linear relationship between frequency and mass (i.e. Sauerbrey equation) remains true in our study. A comparison of $K_L$ values in the two substrates suggests that the affinity parameter of CBM1 on NCC and NFC films is significantly different. The former is almost three folds over the latter, which may be attributed to the difference of porosity and roughness of cellulose films, and crystallinity of two cellulose substrates. Previous studies (Alekozai et al. 2014) have shown that CBM1 is more easily adsorbed on the hydrophobic surface of crystalline cellulose. Our results also confirmed that cellulose substrate with higher crystallinity (i.e. NCC) has a higher affinity to CBM1.

In a conclusion, the surface area or roughness of the films that provides the accessible area for CBM1 adsorption may contribute more to $Q_m$, while the affinity between CBM1 and substrate contributes more to $K_L$. It explains why NCC has a better affinity but with a lower maximum adsorption amount than NFC does.

The Freundlich isotherm is often used to describe the multilayer adsorption of multiphase systems. The equation is as Eq. 4:

$$Q_e = K_F C^{1/n} \tag{4}$$

where $Q_e$ is the amount of the CBM1 adsorbed on the cellulose in equilbrium, $K_F$ is the equilibrium adsorption constant, $C$ is the equilibrium concentration of cellulose in the solution, $1/n$ is the heterogeneity coefficient between 0 and 1.

The linear form of Freundlich isotherm is represented as Eq. 5:

$$\lg Q_e = \lg K_F + 1/n \lg C \tag{5}$$

The constant $K_F$ and $1/n$ can be obtained from the slope and intercept of the linear form of Freundlich isotherms. Figure 4b showed the Freundlich isotherms of CBM1 on NFC and NCC films at 25 °C. The values of constant $K_F$ and $1/n$ were calculated and summarized in Table 1. The $K_F$ values expressed in frequency, were 13.32 and 12.91 Hz $mg^{-1/n}L^{1/n}$, respectively for the adsorption on NCC and NFC films, which equivalent to 2.246 and 1.653 $\mu$mol $g^{-1-1/n}L^{1/n}$. The $1/n$ value for the adsorption on NCC was 0.476 ± 0.002, which was significantly lower than that of NFC 0.697 ± 0.003. The goodness-of-fit for the adsorption of CBM1 on NFC and NCC films fitted by Freundlich model is all above 0.98.

## Evaluation of the preferential binding

Free energy changes ($\Delta G$) can be calculated from the following equation Eq. 6.

$$\Delta G = -RT \ln K_L \tag{6}$$

where $T$ is the temperature (K), $R$ is gas constant (J $Kmol^{-1}$), $K_L$ is the constants (L $mg^{-1}$) obtained from Langmuir model. The Gibbs free energy for adsorption of CBM1 on NCC and NFC films is calculated to be $-25.60 \pm 0.01$ and $-23.70 \pm 0.03$ kJ $mol^{-1}$, respectively.

The Gibbs free energy calculated for the two cellulose substrates were both negative, suggesting the spontaneous nature of the interaction between CBM1 and cellulose film. In addition, the Gibbs free energy of NCC is more negative than that of NFC, indicating that CBM1 prefers to bind on NCC rather than on NFC. It is because NCC contains mainly the crystalline regions of cellulose and NFC contains both crystalline and amorphous regions of cellulose and with a more porous structure.

Arola and Linder (2016) measured the $\Delta G$ for the CBM from Cel6A and Cel7A for both NFC and bacterial cellulose by determining the free $^3$H-labled protein after adsorption via liquid scintillation. Their results are in the range of $-30$ to $-25$ kJ $mol^{-1}$. They also measured the $\Delta G$ for the enzymes with two CBMs and reported a range of $-34$ to $-30$ kJ $mol^{-1}$. Regard to the CBMs from other families, the $\Delta G$ of CBM17 binding to cello-oligosaccharides for soluble polysaccharides for wild-type and mutants is in the range of $-17$ to $-27$ kJ $mol^{-1}$ (Tomme et al. 2000); the $\Delta G$ of CBM27 binding to mannooligosaccharides at 25 °C in 50 mM Potassium Phosphate Buffer (pH 7.0) is in the range of $-21.36$ to $-34.99$ kJ $mol^{-1}$ (Lammerts van Bueren and Boraston 2004). Our results on Gibbs free energy obtained from the isotherms by QCM technique are in a good agreement with the literature values.

## Conclusions

This study investigated the adsorption behaviors of the isolated CBM1 with a range of concentrations onto NCC and NFC films using a QCM-D technique. All the adsorption curves can be fitted by both Langmuir and Freundlich models. In the Langmuir fitting, $Q_m$ is $-144.7$ Hz (0.02469 mmol $g^{-1}$) and $-482.3$ Hz (0.05988 mmol $g^{-1}$) for the adsorption of CBM1 on NCC and NFC films, respectively, while $K_L$ is $0.03072 \pm 0.00017$ and $0.01427 \pm 0.00014$ L $mg^{-1}$, accordingly. In the Freundlich fitting, $K_F$ is 13.32 Hz $mg^{-1/n}L^{1/n}$ (0.002246 nmol $g^{-1-1/n}L^{1/n}$) and 12.91 Hz $mg^{-1/n}L^{1/n}$ (0.001653 nmol $g^{-1-1/n}L^{1/n}$), while parameter $1/n$ is $0.476 \pm 0.002$ and $0.697 \pm 0.003$, respectively. Gibbs free energy derived from the $K_L$ of Langmuir model, $-25.60 \pm 0.01$ and $-23.70 \pm 0.03$ kJ $mol^{-1}$. In view of the $K_L$ in the Langmuir fitting, the $1/n$ in the Freundlich fitting and Gibbs free energy obtained, the results show that CBM1 has a preferential binding to the NCC film than NFC film.

**Acknowledgments** This project was financially supported by the National Natural Science Foundation of China (Nos. 31730106, 31270613 and 31770623), the Natural Science Foundation of Jiangsu Provincial Universities (No. 17KJA530005), Qing-Lan Projects, and the Priority Academic Program Development of Jiangsu Higher Education Institutions. We are very grateful to Yan V. Li at Colorado State University for English editing.

## References

Ahola S, Salmi J, Johansson LS, Laine J, Osterberg M (2008a) Model films from native cellulose nanofibrils. Preparation, swelling, and surface interactions. Biomacromolecules 9(4):1273–1282

Ahola S, Turon X, Osterberg M, Laine J, Rojas OJ (2008b) Enzymatic hydrolysis of native cellulose nanofibrils and other cellulose model films: effect of surface structure. Langmuir 24(20):11592–11599

Alekozai EM, GhattyVenkataKrishna PK, Uberbacher EC, Crowley MF, Smith JC, Cheng X (2014) Simulation analysis of the cellulase Cel7A carbohydrate binding module on the surface of the cellulose Iβ. Cellulose 21(2):951–971

Arola S, Linder MB (2016) Binding of cellulose binding modules reveal differences between cellulose substrates. Sci Rep 6:35358

Beck-Candanedo S, Roman M, Gray DG (2005) Effect of reaction conditions on the properties and behavior of wood cellulose nanocrystal suspensions. Biomacromolecules 6(2):1048–1054

Beckham GT, Matthews JF, Bomble YJ, Bu L, Adney WS, Himmel ME, Nimlos MR, Crowley MF (2010) Identification of amino acids responsible for processivity in a family 1 carbohydrate-binding module from a fungal cellulase. J Phys Chem B 114(3):1447–1453

Boraston AB (2005) The interaction of carbohydrate-binding modules with insoluble non-crystalline cellulose is enthalpically driven. Biochem J 385:479–484

Boraston AB, Nurizzo D, Notenboom V, Ducros V, Rose DR, Kilburn DG, Davies GJ (2002) Differential oligosaccharide recognition by evolutionarily-related beta-1,4 and beta-1,3 glucan-binding modules. J Mol Biol 319(5):1143–1156

Boraston AB, Revett TJ, Boraston CM, Nurizzo D, Davies GJ (2003) Structural and thermodynamic dissection of specific

mannan recognition by a carbohydrate binding module, TmCBM27. Structure 11(6):665–675
Boraston AB, Bolam DN, Gilbert HJ, Davies GJ (2004) Carbohydrate-binding modules: fine-tuning polysaccharide recognition. Biochem J 382:769–781
Ciolacu D, Kovac J, Kokol V (2010) The effect of the cellulose-binding domain from Clostridium cellulovorans on the supramolecular structure of cellulose fibers. Carbohydr Res 345(5):621–630
Ciolacu D, Chiriac AI, Pastor FIJ, Kokol V (2014) The influence of supramolecular structure of cellulose allomorphs on the interactions with cellulose-binding domain, CBD3b from Paenibacillus barcinonensis. Bioresour Technol 157:14–21
Creagh AL, Ong E, Jervis E, Kilburn DG, Haynes CA (1996) Binding of the cellulose-binding domain of exoglucanase Cex from Cellulomonas fimi to insoluble microcrystalline cellulose is entropically driven. Proc Natl Acad Sci USA 93(22):12229–12234
Dagel DJ, Liu Y-S, Zhong L, Luo Y, Himmel ME, Xu Q, Zeng Y, Ding S-Y, Smith S (2011) In situ imaging of single carbohydrate-binding modules on cellulose microfibrils. J Phys Chem B 115(4):635–641
Eriksson J, Malmsten M, Tiberg F, Callisen TH, Damhus T, Johansen KS (2005) Model cellulose films exposed to H. insolens glucoside hydrolase family 45 endo-cellulase—the effect of the carbohydrate-binding module. J Colloid Interface Sci 285(1):94–99
Fält S, Wågberg L, Vesterlind E-L (2003) Swelling of model films of cellulose having different charge densities and comparison to the swelling behavior of corresponding fibers. Langmuir 19(19):7895–7903
Flint J, Nurizzo D, Harding SE, Longman E, Davies GJ, Gilbert HJ, Bolam DN (2004) Ligand-mediated dimerization of a carbohydrate-binding module reveals a novel mechanism for protein-carbohydrate recognition. J Mol Biol 337(2):417–426
Garg A, Heflin JR, Gibson HW, Davis RM (2008) Study of film structure and adsorption kinetics of polyelectrolyte multilayer films: effect of pH and polymer concentration. Langmuir 24(19):10887–10894
Guillen D, Sanchez S, Rodriguez-Sanoja R (2010) Carbohydrate-binding domains: multiplicity of biological roles. Appl Microbiol Biotechnol 85(5):1241–1249
Hasan M, Ahmad A, Hameed B (2008) Adsorption of reactive dye onto cross-linked chitosan/oil palm ash composite beads. Chem Eng J 136(2):164–172
Hervé C, Rogowski A, Blake AW, Marcus SE, Gilbert HJ, Knox JP (2010) Carbohydrate-binding modules promote the enzymatic deconstruction of intact plant cell walls by targeting and proximity effects. Proc Natl Acad Sci USA 107(34):15293–15298
Hu G, Heitmann JA, Rojas OJ (2009) Quantification of cellulase activity using the quartz crystal microbalance technique. Anal Chem 81(5):1872–1880
Hu F, Zhang Y, Wang P, Wu S, Jin Y, Song J (2018) Comparison of the interactions between fungal cellulases from different origins and cellulose nanocrystal substrates with different polymorphs. Cellulose 25(2):1185–1195
Jiang C, Cao T, Wu W, Song J, Jin Y (2017) A novel approach to prepare ultrathin lignocellulosic film for monitoring enzymatic hydrolysis process by quartz crystal microbalance. ACS Sustain Chem Eng 5(5):3837–3844
Jin E, Guo J, Yang F, Zhu Y, Song J, Jin Y, Rojas OJ (2016) On the polymorphic and morphological changes of cellulose nanocrystals (CNC-I) upon mercerization and conversion to CNC-II. Carbohydr Polym 143:327–335
Jin E, Zhang Y, Hu F, Yang F, Wu S, Jin Y, Song J (2017) To understand the superior hydrolytic activity after polymorphic conversion from cellulose I to II from the adsorption behaviors of enzymes. Cellulose 24(3):1371–1381
Josefsson P, Henriksson G, Wågberg L (2007) The physical action of cellulases revealed by a quartz crystal microbalance study using ultrathin cellulose films and pure cellulases. Biomacromolecules 9(1):249–254
Laaksonen P, Walther A, Malho JM, Kainlauri M, Ikkala O, Linder MB (2011) Genetic engineering of biomimetic nanocomposites: diblock proteins, graphene, and nanofibrillated cellulose. Angew Chem Int 50(37):8688–8691
Lammerts van Bueren A, Boraston AB (2004) Binding sub-site dissection of a carbohydrate-binding module reveals the contribution of entropy to oligosaccharide recognition at "non-primary" binding subsites. J Mol Biol 340(4):869–879
Lehtio J, Sugiyama J, Gustavsson M, Fransson L, Linder M, Teeri TT (2003) The binding specificity and affinity determinants of family 1 and family 3 cellulose binding modules. Proc Natl Acad Sci USA 100(2):484–489
Linder M, Teeri TT (1997) The roles and function of cellulose-binding domains. J Biotechnol 57(1–3):15–28
Liu Y-S, Baker JO, Zeng Y, Himmel ME, Haas T, Ding S-Y (2011) Cellobiohydrolase hydrolyzes crystalline cellulose on hydrophobic faces. J Biol Chem 286(13):11195–11201
Martin-Sampedro R, Rahikainen JL, Johansson L-S, Marjamaa K, Laine J, Kruus K, Rojas OJ (2013) Preferential adsorption and activity of monocomponent cellulases on lignocellulose thin films with varying lignin content. Biomacromolecules 14(4):1231–1239
Mattinen M-L, Linder M, Teleman A, Annila A (1997) Interaction between cellohexaose and cellulose binding domains from *Trichoderma reesei* cellulases. FEBS Lett 407(3):291–296
McGuffee SR, Elcock AH (2006) Atomically detailed simulations of concentrated protein solutions: the effects of salt, pH, point mutations, and protein concentration in simulations of 1000-molecule systems. J Am Chem Soc 128(37):12098–12110
Mittal A, Katahira R, Himmel ME, Johnson DK (2011) Effects of alkaline or liquid-ammonia treatment on crystalline cellulose: changes in crystalline structure and effects on enzymatic digestibility. Biotechnol Biofuels 4(1):41
Mittal N, Jansson R, Widhe M, Benselfelt T, Håkansson KM, Lundell F, Hedhammar M, Söderberg LD (2017) Ultrastrong and bioactive nanostructured bio-based composites. ACS Nano 11(5):5148–5159
Niinivaara E, Faustini M, Tanunelin T, Kontturi E (2015) Water vapor uptake of ultrathin films of biologically derived nanocrystals: quantitative assessment with quartz crystal microbalance and spectroscopic ellipsometry. Langmuir 31(44):12170–12176
Nimlos MR, Beckham GT, Matthews JF, Bu L, Himmel ME, Crowley MF (2012) Binding preferences, surface

attachment, diffusivity, and orientation of a family 1 carbohydrate-binding module on cellulose. J Biol Chem 287(24):20603–20612

Notenboom V, Boraston AB, Chiu P, Freelove ACJ, Kilburn DG, Rose DR (2001) Recognition of cello-oligosaccharides by a family 17 carbohydrate-binding module: an X-ray crystallographic, thermodynamic and mutagenic study. J Mol Biol 314(4):797–806

Nussinovitch A, Shpigel E, Shoseyov O (2002) Recombinant cellulose crosslinking protein: a novel paper-modification biomaterial. Cellulose 9(1):91–98

Palonen H, Tenkanen M, Linder M (1999) Dynamic interaction of *Trichoderma reesei* cellobiohydrolases Cel6A and Cel7A and cellulose at equilibrium and during hydrolysis. Appl Environ Microbiol 65(12):5229–5233

Pellegrini VO, Lei N, Kyasaram M, Olsen JP, Badino SF, Windahl MS, Colussi F, Cruys-Bagger N, Borch K, Westh P (2014) Reversibility of substrate adsorption for the cellulases Cel7A, Cel6A, and Cel7B from Hypocrea jecorina. Langmuir 30(42):12602–12609

Rodahl M, Hook F, Krozer A, Brzezinski P, Kasemo B (1995) Quartz-crystal microbalance setup for frequency and Q-factor measurements in gaseous and liquid environments. Rev Sci Instrum 66(7):3924–3930

Sakka K, Nakanishi M, Sogabe M, Arai T, Ohara H, Tanaka A, Kimura T, Ohmiya K (2003) Isothermal titration calorimetric studies on the binding of a family 6 carbohydrate-binding module of *Clostridium thermocellum* XynA with xylooligosaccharides. Biosci Biotechnol Biochem 67(2):406–409

Sauerbrey G (1959) The use of quartz oscillators for weighing thin layers and for microweighing. Z Angew Phys 155(2):206–222

Seo D-J, Fujita H, Sakoda A (2011) Structural changes of lignocelluloses by a nonionic surfactant, Tween 20, and their effects on cellulase adsorption and saccharification. Bioresour Technol 102(20):9605–9612

Shen F, Rojas OJ, Genzer J, Gurgel PV, Carbonell RG (2016) Affinity interactions of human immunoglobulin G with short peptides: role of ligand spacer on binding, kinetics, and mass transfer. Anal Bioanal Chem 408(7):1829–1841

Song JL, Liang J, Liu XM, Krause WE, Hinestroza JP, Rojas OJ (2009) Development and characterization of thin polymer films relevant to fiber processing. Thin Solid Films 517(15):4348–4354

Song JL, Yamagushi T, Silva DJ, Hubbe MA, Rojas OJ (2010) Effect of charge asymmetry on adsorption and phase separation of polyampholytes on silica and cellulose surfaces. J Phys Chem B 114(2):719–727

Song J, Yang F, Zhang Y, Hu F, Wu S, Jin Y, Guo J, Rojas OJ (2017) Interactions between fungal cellulases and films of nanofibrillar cellulose determined by a quartz crystal microbalance with dissipation monitoring (QCM-D). Cellulose 24(5):1947–1956

Sorensen TH, Cruys-Bagger N, Borch K, Westh P (2015a) Free energy diagram for the heterogeneous enzymatic hydrolysis of glycosidic bonds in cellulose. J Biol Chem 290(36):22203–22211

Sorensen TH, Cruys-Bagger N, Windahl MS, Badino SF, Borch K, Westh P (2015b) Temperature effects on kinetic parameters and substrate affinity of Cel7A cellobiohydrolases. J Biol Chem 290(36):22193–22202

Tammelin T, Saarinen T, Österberg M, Laine J (2006) Preparation of Langmuir/Blodgett-cellulose surfaces by using horizontal dipping procedure. Application for polyelectrolyte adsorption studies performed with QCM-D. Cellulose 13(5):519–535

Tammelin T, Johnsen IA, Österberg M, Stenius P, Laine J (2007) Adsorption of colloidal extractives and dissolved hemicelluloses on thermomechanical pulp fiber components studied by QCM-D. Nord Pulp Pap Res J 22(1):93–101

Tomme P, Boraston A, Kormos JM, Warren RAJ, Kilburn DG (2000) Affinity electrophoresis for the identification and characterization of soluble sugar binding by carbohydrate-binding modules. Enzyme Microb Technol 27:453–458

Tsiamis A, Taylor SE (2017) Adsorption behavior of asphaltenes and resins on kaolinite. Energy Fuels 31(10):10576–10587

Turon X, Rojas OJ, Deinhammer RS (2008) Enzymatic kinetics of cellulose hydrolysis: a QCM-D study. Langmuir 24(8):3880–3887

Voinova MV, Rodahl M, Jonson M, Kasemo B (1999) Viscoelastic acoustic response of layered polymer films at fluid-solid interfaces: continuum mechanics approach. Phys Scr 59(5):391–396

Xu K, Ouberai MM, Welland ME (2013) A comprehensive study of lysozyme adsorption using dual polarization interferometry and quartz crystal microbalance with dissipation. Biomaterials 34(5):1461–1470

Yui T, Shiiba H, Tsutsumi Y, Hayashi S, Miyata T, Hirata F (2010) Systematic docking study of the carbohydrate binding module protein of Cel7A with the cellulose I alpha crystal model. J Phys Chem B 114(1):49–58